

The influence of flow electrode channel design on flow capacitive deionization performance: Experimental and CFD modelling insights

H.M. Saif^a, T.H. Gebregeorgis^{a,1}, J.G. Crespo^{a,b}, S. Pawlowski^{a,*}

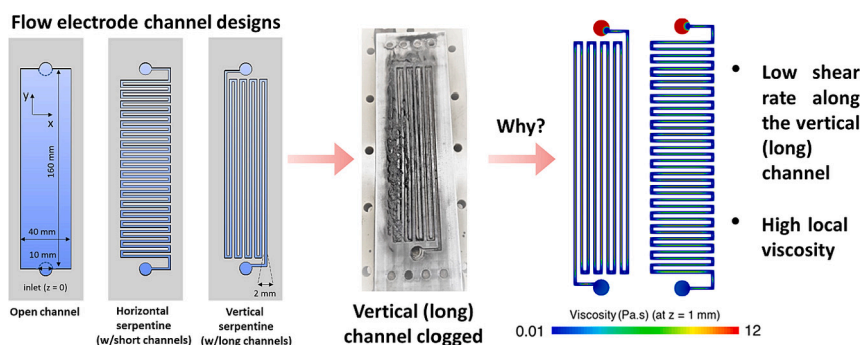
^a LAQV-REQUIMTE, DQ, FCT, Universidade NOVA de Lisboa, 2829-516 Caparica, Portugal

^b Instituto de Tecnologia Química e Biológica António Xavier, Universidade Nova de Lisboa, Av. da República, 2780-157 Oeiras, Portugal

HIGHLIGHTS

- PET-G 1.75 mm filament was used to 3D print different flow electrode channels.
- Vertical serpentine channels blocked with flow electrodes' carbon particles.
- The best FCDI performance was achieved when using horizontal serpentine channels.
- Not even horizontal serpentine channels promoted adequate internal mixing.
- Channels' geometry affects flow electrodes' local viscosity and, therefore, FCDI performance.

GRAPHICAL ABSTRACT



ARTICLE INFO

Keywords:

Flow capacitive deionization (FCDI)
3D printing
Rheology of flow electrodes
Clogging
Computational fluid dynamics (CFD)

ABSTRACT

Flow capacitive deionization (FCDI) is an emerging desalination technology at which flow electrodes (shear-thinning flowable carbon slurries) are used to remove ions from saline water. The geometry of flow electrode channels, which provide the path and ensure the distribution and mixing of the flow electrodes, is one of the most important aspects to be optimized. This work presents experimental and computational fluid dynamics (CFD) modelling analysis of the influence of the geometry of flow electrode channels on FCDI performance. Flow electrode gaskets (with open, serpentine (short) horizontal and serpentine (long) vertical channels) were 3D printed using a polyethylene terephthalate glycol (PET-G) filament. The FCDI cell with a vertical serpentine flow electrode channel exhibited the poorest performance due to channel blockage by carbon particles, while the best results were achieved with a horizontal serpentine flow electrode channel. CFD simulations aided in understanding this behaviour by showing that the channel geometry strongly affects the local shear rate, and thus the local viscosity of flow electrodes. Thus, it is recommended to design channels that induce flow disturbance aiming for increasing the shear rate and hence reducing flow electrode viscosity, therefore promoting their flowability and reducing clogging chances.

* Corresponding author.

E-mail address: s.pawlowski@fct.unl.pt (S. Pawlowski).

¹ Current address: Research Group Electrochemical and Surface Engineering (SURF), Department of Materials and Chemistry, Vrije Universiteit Brussel (VUB), Pleinlaan 2, 1050 Brussels, Belgium.

<https://doi.org/10.1016/j.desal.2024.117452>

Received 21 October 2023; Received in revised form 12 January 2024; Accepted 18 February 2024

Available online 21 February 2024

0011-9164/© 2024 The Authors. Published by Elsevier B.V. This is an open access article under the CC BY-NC-ND license (<http://creativecommons.org/licenses/by-nc-nd/4.0/>).

1. Introduction

Flow Capacitive Deionization (FCDI) is an electro-membrane desalination technology proposed in 2013 [1]. This technology employs flow electrodes to extract ions from saline streams by their electro-sorption at micropores of carbon particles composing flow electrodes [2]. Recently, FCDI has also been explored for selective recovery of target ions such as lithium [3] and ammonia [4]. The conventional FCDI cell consists of endplates, current collectors (both anode and cathode) and ion-exchange membranes separated by spacers. Typically, flow electrodes are circulated within the channels engraved on the surfaces of current collectors made of graphite or stainless-steel plates [5]. The formation of an electrical double layer (EDL) on the surfaces of carbon particles occurs when an electrical potential difference is applied between current collectors. This EDL leads to the capacitive electro-sorption of ions [1,6].

Flow electrodes should be made of highly conductive and capacitive materials, with low viscosity, to ensure efficient ion adsorption while being easily circulated through the flow electrode channels [7,8]. The addition of conductive additives to carbon slurries increases flow electrode conductivity, thus decreasing the internal electric resistance, but also increases the final fluid viscosity [9,10]. Thus, the choice of active materials, conductive additives, and electrolytes composing the flow electrode is paramount [11]. In general, activated carbon slurries are used as flow electrodes, which can be recirculated and regenerated *in-situ*, ensuring an energetically efficient process [12,13]. These carbon slurries have a shear thinning behaviour, meaning that their viscosity decreases with the increase of shear rate [9]. The shear rate, which corresponds to the gradient in velocity, depends on system geometry and fluid dynamics. To date, mostly serpentine-type channels have been used in FCDI cells to distribute and mix the flow electrodes [14–16]. There are very few studies in which other flow channel designs were explored and compared with the serpentine one [17]. The widening of these channels varies from 1 mm to 4 mm, and the most used width is 2 mm [1,8,11,14,18–21]. Furthermore, since FCDI is still in its infancy, the so far performed studies were carried out in small devices and, thus, many crucial questions regarding the improvement of flow electrode channel design such as how the length and width of these channels affect the performance and clogging of the FCDI system remain unanswered.

In this work, the impact of flow electrode channel design on the efficiency of flow-electrode capacitive deionization (FCDI) systems was thoroughly examined in terms of achieved salt removal (from brackish water), as well as through the assessment of flow electrode distribution, flowability, mixing and pressure drop. To obtain empirical insights, flow electrode gaskets with different channel designs (open, serpentine horizontal, and serpentine vertical) were prepared using 3D printing technology which is a simple and fast prototyping (manufacturing) technique in contrast to traditional CNC milling [22]. These gaskets were then integrated within FCDI cells and desalination tests under zero-voltage desorption (ZVD) and reversed-voltage (RVD) desorption conditions were performed. To further understand the complex fluidic phenomena occurring within various channel designs, including their clogging, computational fluid dynamics (CFD) simulations were performed, disclosing a significant impact of channel geometry/dimensions on the local shear rate values and, thus on the local viscosity of flow electrodes. Based on experimental and CFD modelling results, guidelines for the design of flow electrode channels were derived.

2. Materials and methods

2.1. Materials

Polyethylene terephthalate glycol (PET-G) 1.75 mm filament (Dowire®, Portugal) was used to prepare the flow electrode gaskets by a 3D printer. A stick adhesive (AprintaPro PrintaStick, 50 mL) was used to stick the filament to the printer bed. Powder activated carbon (AC), purchased from José M. Vaz Pereira LDA, Lisbon, Portugal, was used to

prepare flow electrodes. NaCl salt (Honeywell Fluka™ Chemicals, Germany) was used to prepare the electrolyte and feed solution. Milli-Q water (Millipore), with approximately 19 MΩ cm, was used to prepare all solutions.

2.2. Preparation of flow electrode gaskets (3D printing)

3D printing is an additive manufacturing technology that allows for creating 3-dimensional solid objects. One of the greatest advantages of 3D printing is its flexibility, low cost and ability to fabricate objects with the desired/customised geometry [23]. The fused deposition modelling (FDM) 3D printing technique based on the extrusion of thermoplastic materials in a layer-by-layer fashion was used to manufacture flow electrode gaskets and create the respective flow electrode channels. The gaskets (Fig. 1) were designed using computer-aided design (CAD) Autodesk Fusion 360 software.

Three different geometries were drawn: open (empty), serpentine horizontal and serpentine vertical. The open flow area was 6400 mm² (160 × 40 mm). The horizontal serpentine geometry contained 36 evenly spaced 2 × 2 mm square cross section and 34 mm long segments, whereas the vertical serpentine geometry contained 7 evenly spaced 2 × 2 mm square cross section and 142 mm long segments, except for channels connected with inlet and outlet, which were 149 mm long. The contact area between membrane and flow-electrode channel in both serpentine designs was 2658 mm². The geometry of these three gaskets was saved in the appropriate file format of Standard Tessellation Language (.STL) followed by a slicing technique done by Voxelizer software to translate .STL files into instructions for a multitool ZMorph 3D printer through a generation of a G-code. Polyethylene terephthalate glycol (PET-G) 1.75 mm filament (Dowire®, Portugal) was used to print gaskets, and a print stick adhesive (AprintaPro PrintaStick, 50 mL) to improve adhesion of the first printed layer to the printer bed. PET-G is an amorphous plastic in which glycol is added to PET to avoid the overheating limitation of PET and to minimize its brittleness and fragility. This filament is broadly used in the additive manufacturing market, combining the strength of acrylonitrile butadiene styrene (ABS) and polylactic acid (PLA) filaments. It has excellent thermal stability and is relatively easy to extrude. The 3D printer was first calibrated to manufacture the best quality prints by making several tests when printing the horizontal serpentine gaskets since they were the first ones to be produced. Some of the tested FDM printing parameters were extrusion temperature, bed temperature and printing speed. Once the 3D printing of gaskets was finished, a post-processing (refining) step was carried out; they were cleaned and polished with sandpaper to smoothen their surface.

2.3. Assembling of flow capacitive deionization (FCDI) cell

The FCDI cell (with one feed compartment and two flow electrode compartments) was assembled by adapting endplates and spacers from the EDR-Z-Mini electrodialysis unit (MEGA, Czech Republic) [24,25]. The endplates with embedded 210 × 60 mm (length and width) platinum-coated titanium electrodes were used as current collectors, while spacers were used to create the 0.8 mm thick feed channel. The flow-electrode compartments were created by using different 3D printed PET-G gaskets. MIARCO® polytetrafluoroethylene (PTFE) Teflon tape of 12 mm × 0.075 mm (width x thickness) was used to prevent water leakages and to seal the flow electrode channels. A Fumasep® FAB-PK-130 anion-exchange membrane was placed between the feed channel and the anode compartment, and a Fumasep® FKB-PK-130 cation-exchange membrane was placed between the feed channel and the cathode compartment. Each ion exchange membrane, both supplied by Fumatech GmbH, Germany, had a thickness of 150 μm.

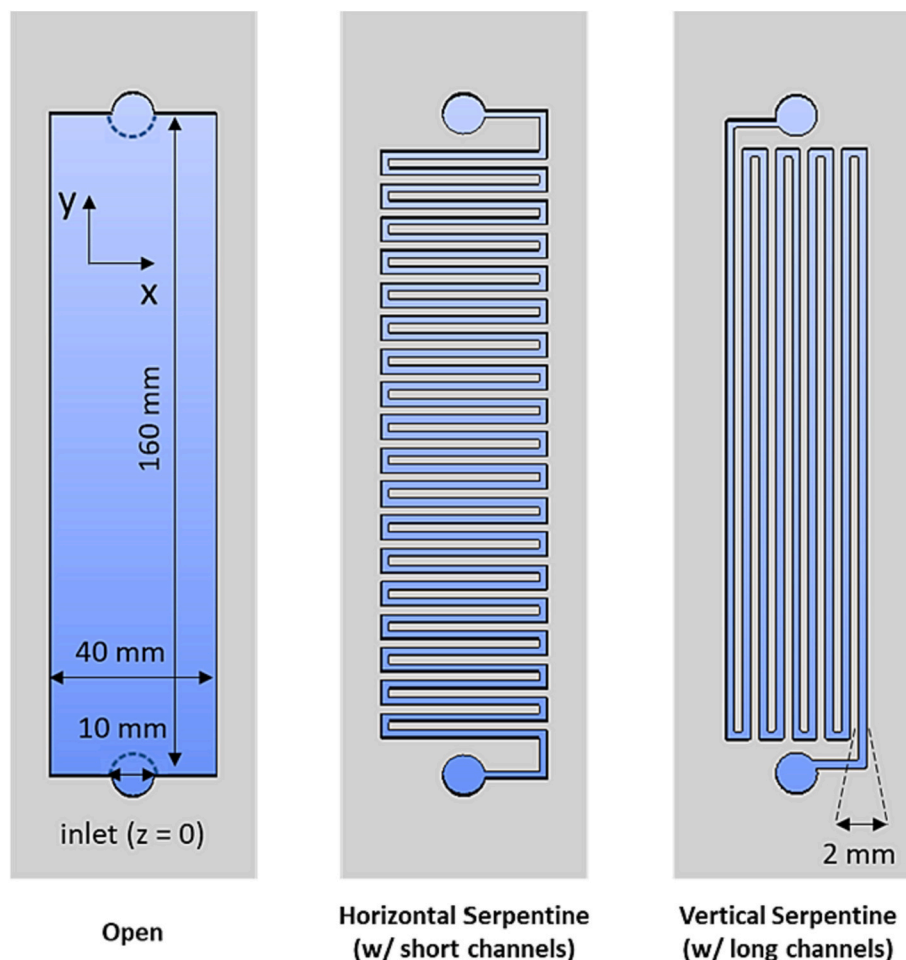


Fig. 1. CAD design of gaskets forming flow-electrodes' channels: (from left to right) open, horizontal serpentine and vertical serpentine.

2.4. Desalination tests

A Vertex.5A potentiostat (Ivium Technologies, The Netherlands) was used as power source. In all the desalination tests, 1.5 g/L NaCl solution (brackish water feed stream) was pumped to the FCDI cell at a flow rate of 10 mL/min using a peristaltic pump (Lead Fluid – BT100S, China). The conductivity of the effluent was measured at the exit of the FCDI cell every 2 s using a conductivity meter (Horiba Laqua-PC1100, Japan). The flow electrodes were prepared by dispersing activated carbon (AC) in 1 g/L NaCl aqueous solution (50 mL). A beaker cup containing the solution was covered by aluminium foil paper to prevent water evaporation and then slightly heated and stirred during 24 h using a mixer (Velp Scientific OHS 100 Digital Overhead Stirrer) to attain a uniform carbon dispersion. Flow electrodes with 0 wt% (just 1 g/L NaCl solution), 5 wt%, 10 wt% and 15 wt% of AC were prepared. In all desalination tests, the flow electrodes were circulated in separated anodic and cathodic closed-loop circuits at the flow rate of 60 mL/min using a peristaltic pump (Masterflex® L/S® Digital Peristaltic Pump Drive, UK). The pressure drop in flow electrode channels was measured using two pressure sensors (Range 0–2.5 bar, CIT-F-I2, Prignitz Mikrosystemtechnik, Germany) one installed at the inlet and the other at the outlet of FCDI cells.

At first, to investigate the effect of carbon loading (please see Supplementary Information, section 3), flow electrodes with 0, 5, 10 and 15 wt% of AC, were used in desalination tests performed in a single pass mode, at ± 1 V, thus at reverse voltage desorption (RVD) conditions, and cycling time step of 150 s. The horizontal serpentine channel flow electrode gaskets were used in those tests.

Afterwards, to assess the influence of different flow electrode

channels' design at the performance of FCDI, flow electrodes with 10 wt% of AC were used at desalination tests with open, serpentine vertical and serpentine horizontal channels gaskets carried out for five consecutive cycles of charging and discharging of 300 s each in a single-pass method at 1.2 V and zero-voltage (ZVD) and reverse-voltage (RVD) desorption conditions (Fig. 2 and Figs. SI.1 and SI.2 in the Supplementary Information show the experimental setup).

Salt removal (Γ) and salt adsorption capacity (SAC) (mg of salt /g of carbon at both electrodes) were calculated using the following equations:

$$\Gamma = \int_0^{t, \text{charge}} Q(c, \text{feed} - c, \text{effluent}) dt \quad (1)$$

$$\text{SAC} = \Gamma * M_{\text{salt}} / m_{\text{electrodes}} \quad (2)$$

where Q is the feedwater flow rate, c is the concentration, t is the time, M_{salt} is the molar mass of salt and $m_{\text{electrodes}}$ is the total mass of active carbon material (both electrodes).

2.5. Computational fluid dynamics (CFD) simulations

To elucidate the impact of each studied flow electrode channel geometry (and specifically the reason for the clogging of the serpentine vertical channels), the flow fields in flow electrode channels were simulated using an open-source CFD software (OpenFOAM, v.7, <https://openfoam.org>). The snappyHexMesh OpenFOAM grid generation utility (<https://cfd.direct/openfoam/user-guide/snappyhexmesh/>) was used to create a computational mesh from the CAD drawings used to

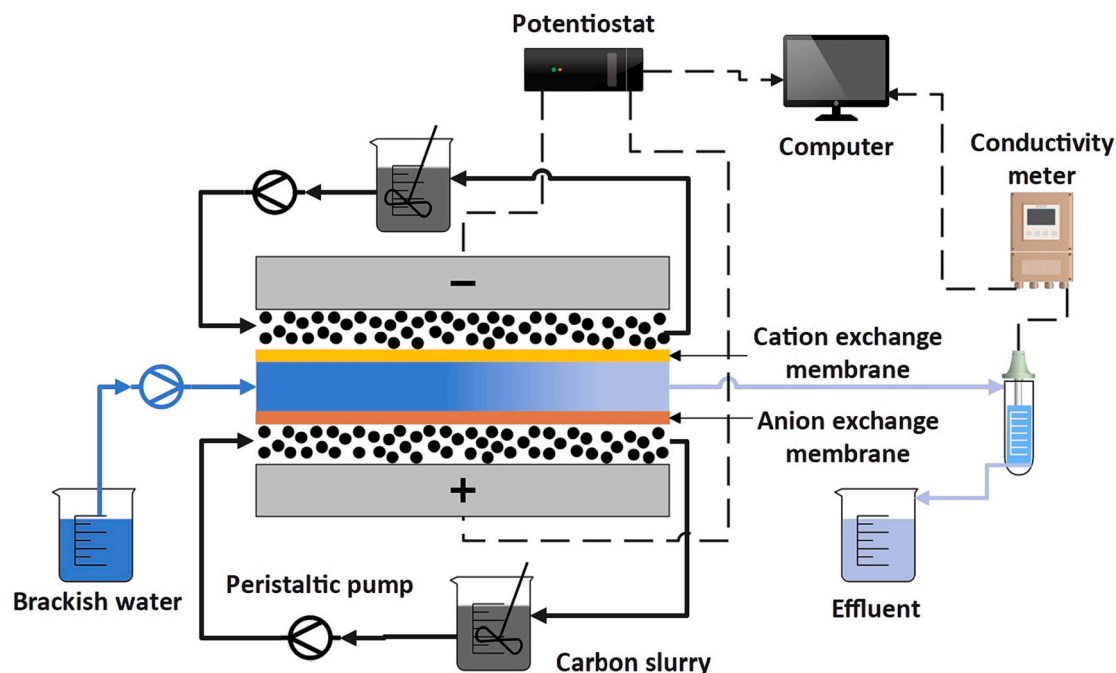


Fig. 2. Schematic representation of the FCDI set up used in desalination tests.

print flow electrode channels gaskets. The mass continuity and Navier-Stokes equations were solved using the SIMPLE (semi-implicit method for pressure-linked equations) algorithm, at the laminar regime, and 15,000 iterations were performed to grant numerical stability (steady state) of the velocity, pressure and viscosity fields. Furthermore, the fluid streamlines were computed using the Paraview 5.3.0 software to visualise the fluid path in the studied computational domains.

Since carbon slurries (such as the flow electrodes used in this study) are non-Newtonian fluids with a shear-thinning behaviour, their apparent viscosity at various shear rates was modelled using the Ostwald–de Waele power law (Eq. (3)) [9,26]:

$$\eta = k \cdot \dot{\gamma}^{n-1} \quad (3)$$

where η is apparent viscosity (Pa.s), k is the consistency index (Pa.sⁿ), $\dot{\gamma}$ is the shear rate (s⁻¹) and n is the shear thinning index (-).

The flow of two fluids was simulated: a) water, which is a Newtonian fluid, thus with constant viscosity, b) flow electrode with 20 wt% of the YP50F activated carbon, which is a non-Newtonian fluid with shear-thinning behaviour (as any flow electrode). YP50F was chosen for the CFD case study since it is one of the most used carbon materials for electric-double layer capacitors, and its k and n values for a 20 wt% suspension were already reported (10.4 Pa.sⁿ and 0.166, respectively [9]).

3. Results and discussion

3.1. 3D printed gaskets

A PET-G thermoplastic material made up of polyethylene terephthalate (PET) and ethylene glycol was used to prepare the gaskets forming flow electrode channels. First, the optimization of 3D printing parameters was performed when manufacturing the horizontal serpentine gaskets. Table SI.1 shows some examples of different nozzle temperature and printing speed influence on the quality of 3D printed gaskets. For case A, shrinkage from one side when heated deformed the thinner parts of the gasket. Thus, the nozzle temperature was reduced in the following attempts. For case B, the third printed layer failed to attach to the second layer, thus the nozzle temperature was slightly increased,

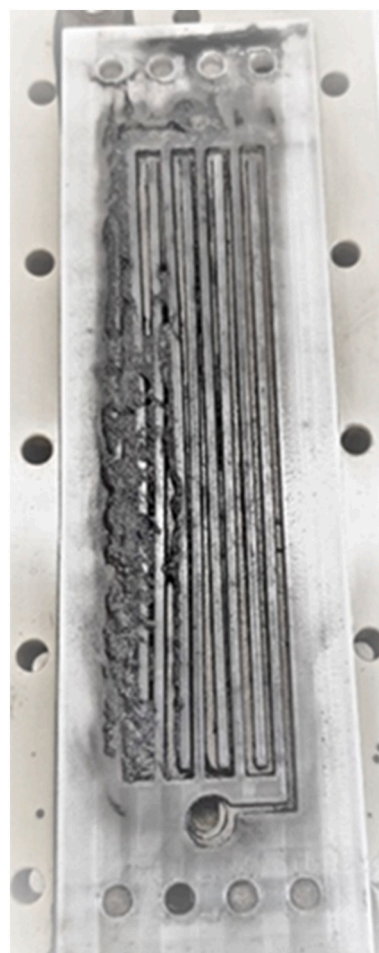


Fig. 3. Vertical serpentine flow electrode channel clogged with carbon particles from flow electrodes.

but kept below the temperature tested in case A. For cases C and D, there were still some problems with the formation of inner channels, thus for case E the infill printing speed was reduced, which allowed to obtain gaskets with the best printing quality. The final optimized FDM parameters set up for printing all PET-G gaskets (open, horizontal serpentine and vertical serpentine) are resumed in Table SI.2 of the Supplementary Information. The time and the length of the filament utilized to print the respective flow electrode channel gaskets are reported in Table SI.3 of the Supplementary Information.

3.2. FCDI desalination tests

Gaskets with three different geometries (open, serpentine vertical and serpentine horizontal) were used to create flow electrode channels in FCDI cells tested for desalination of synthetic brackish water (1.5 g/L NaCl solution).

The flow electrode channel geometry with open gasket allows for the flow of flow electrodes from the inlet to the outlet through all the surface of the current collector. When serpentine gaskets are used, the flow electrodes move in a continuous channel which is zigzagging from inlet to outlet, so there is only one possible flow path. Since the employed current collectors had a rectangular shape with 4 cm of width and 16 cm of length, the segments of the channel which was aligned vertically were

4 times longer than the segments of the channel oriented horizontally. This reduced the number of bends from 35 (in horizontal design) to 8 (in vertical design), which translates into a lower pressure drop (Table SI.4 in Supplementary Information). However, the vertical channels (thus the longer ones) clogged during the performed tests (Fig. 3).

It is possible to see in Fig. 3 that the carbon material accumulated in the middle of the channels, and almost completely blocked the last segment. Such agglomeration of carbon particles affects the efficiency of the FCDI cell because it leads to clogging of the flow electrode channels, and consequently, the FCDI operation has to be interrupted. The reason/mechanism behind vertical channel blocking is discussed in Section 3.3 (CFD simulations) but, shortly, at regions with low shear rate, the viscosity of the flow electrodes increases (due to their shear-thinning behaviour), which decreases the flowability of flow electrodes.

Regarding the desalination tests in the FCDI cell with open and serpentine horizontal channels, the latest performed better (Fig. 4). The electric current passing at the FCDI cell with both kinds of gaskets (open and horizontal serpentine) is almost the same (Fig. 4a and b) even though the quantity of AC carbon and the contact area is 2.4 times higher when using open channels instead of the horizontal serpentine ones. Furthermore, more salt is removed when using the horizontal serpentine channels as seen in Figs. 4c, d and 5. These experimental results suggest that a more efficient transport of ions occurs when using

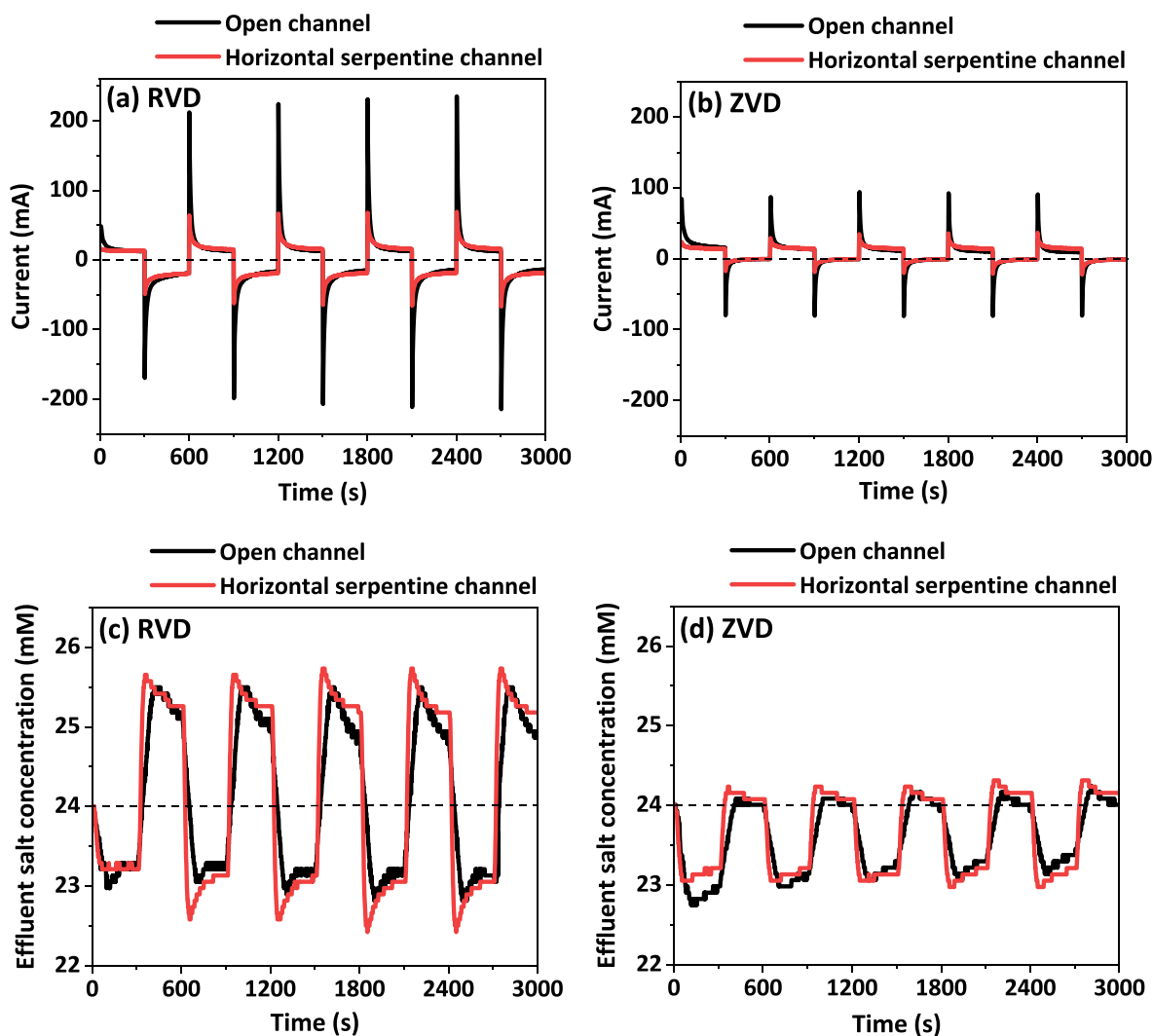


Fig. 4. Chronoamperometric curves at (a) reverse voltage desorption (RVD) conditions (1.2 V and -1.2 V, for adsorption and desorption steps, respectively) and (b) zero voltage desorption (ZVD) conditions (1.2 V and 0 V, for adsorption and desorption steps, respectively); and effluent salt concentration under mentioned RVD and ZVD conditions (c and d, respectively), during desalination of brackish water with 24 mM of NaCl, in FCDI cells with open and horizontal serpentine gaskets.

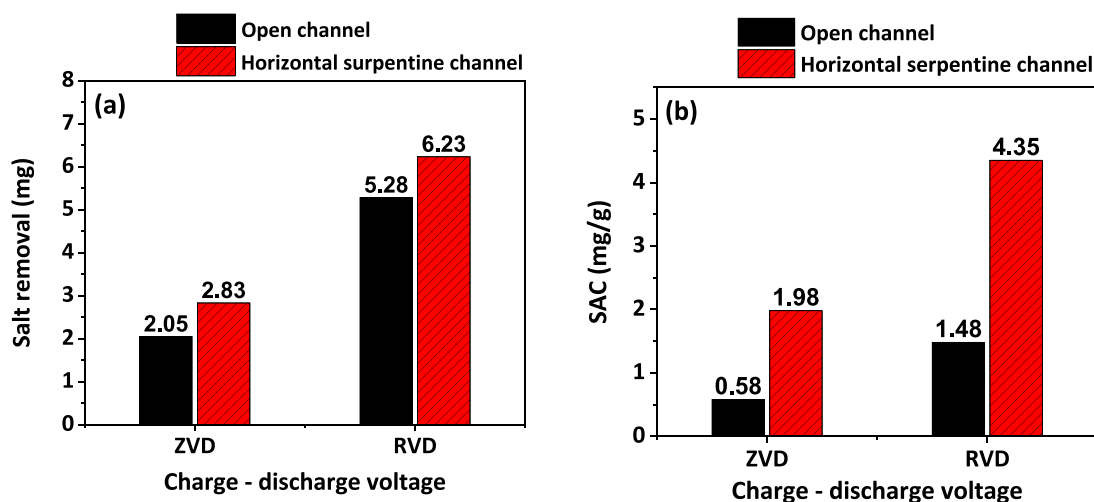


Fig. 5. (a) Salt removal (mg); and (b) Salt adsorption capacity (SAC (mg/g)) at the last, 5th, adsorption step, under RVD and ZVD conditions.

horizontal serpentine channels. The reason why horizontal serpentine channels performed better than the open channel is explained in detail in Section 3.3 (CFD simulations) but, briefly, for the same flow rate, the linear velocity inside the open channel was on average lower than in the serpentine ones, thus the boundary layer resistance was higher, as well as there were dead zones and a higher viscosity region in the middle of the open channel, due to the shear thinning nature of the flow electrode, which hindered the efficient charge percolation.

Regarding the use of two different desorption conditions: reverse voltage desorption (RVD) and zero voltage desorption (ZVD), the performance of FCDI when using the RVD desorption mode was always superior, independently of the kind of employed gasket. When using RVD, a reverse potential difference is applied that helps ions to desorb faster, which regenerates the flow electrodes more effectively during the desorption cycle. In the case of the ZVD mode, the concentration of ions in the effluent was almost the same as in the feed (Fig. 4d), which indicates that the desorption step would need to be performed longer to completely ensure an equivalent ions' desorption. Therefore, for the same adsorption and desorption times, flow electrodes eventually will saturate under the ZVD mode, and their performance will decline over time.

Regarding the salt removal for each case, a more detailed analysis for the last, 5th adsorption step, is shown in Fig. 5. The maximum amount of salt was removed when the horizontal serpentine flow-electrode channels were used under RVD mode (Fig. 5a). This result is in line with the chronoamperometric curves and the effluent salt concentration results. To quantify how efficiently the carbon material was used, the salt adsorption capacity (SAC) achieved during desalination tests was calculated (Fig. 5b). Although SAC is a material property, its value is affected by operating conditions and channel design, which show indirectly that they have a strong effect on the FCDI cell performance. The highest SAC values were always obtained for the horizontal serpentine design, which demonstrates that this design was the most effective to promote flow electrodes capacity to adsorb salts.

3.3. CFD simulations

Computational fluid dynamics (CFD) simulations were performed using open-source OpenFOAM software and the results were visualized using Paraview. CFD simulations were performed to study the flow of water (Newtonian fluid) and a flow electrode (non-Newtonian fluid) in open, serpentine vertical and serpentine horizontal channels employed in the experimental FCDI desalination tests. Fig. 6 shows the velocity fields predicted by CFD simulations of water and 20 wt% YP50F flow electrode at a flow rate of 60 mL/min.

For every case, the computed velocity values are lower when the working fluid is the flow electrode. This is due to a higher viscosity of flow electrodes when compared with water. For the open case, the fluid velocity is constant at almost the entire domain (thus practically without a velocity gradient, except near the walls). At serpentine channels, for water, it is possible to see a gradient of velocity in the channels, with a wide (and higher) velocity region in the middle of channels and decreasing velocity values when approaching walls at which a no-slip condition is observed. For flow electrodes, the only visible velocity profile alterations at serpentine channels are at the bends. However, at the 90° corners, the flow velocity is practically zero, which suggests it would be more attractive to use a more bowed shape.

Since flow electrodes are non-Newtonian fluids with a shear-thinning behaviour and, as seen in Fig. 6, the gradient in velocity is affected by the channel's geometry, the viscosity fields of flow electrodes in different channels were computed. Fig. 7 shows slices of viscosity fields in the middle of the channel thickness for the flow electrode with 20 wt % of YP50F in channels with open, serpentine vertical and serpentine horizontal geometry.

It is possible to observe in Fig. 7 that the viscosity in the serpentine horizontal geometry is lower than in other geometries. Due to the presence of many bends, where the fluid changes its direction 180°, and where the variation of the velocity gradient, thus the shear rate, is higher, the viscosity is lower. Also, the frequent presence of such bends, and short segments between them, prevent that viscosity increases along straight segments. By contrast, in the serpentine vertical design, since straight segments are long, and the bends are few, it is possible to see that the viscosity becomes higher in the straight segments. This higher viscosity, thus lower flowability, explains why in the experimental tests the FCDI cell with serpentine vertical channels was blocked. Widening of vertical channels might delay the clogging issue. Still, as seen in the case of the open channel, which is the maximum case of channel widening, the viscosity becomes extremely high in almost the entire domain. The open channel hasn't clogged (as there was still a pathway for flow electrode flow near the walls), but the performance of the FCDI cell with open channel was worse than with serpentine 2 mm width horizontal channels (Fig. 5). Thus, the widening of the channels might mitigate (or delay) the clogging issue but at the expense of bad mixing and a decrease of shear rate in the middle of the channel, which will increase the viscosity and create a dead zone, without fluid phase renewal, which ultimately might lead to decrease of salt removal. Thus, the introduction of more bends, such as in the horizontal serpentine design, seems to be advisable. To understand in more detail what happens at the bends, fluid streamlines (Fig. 8) were computed from the velocity fields.

Fig. 8 shows streamlines in the channel with open geometry (for

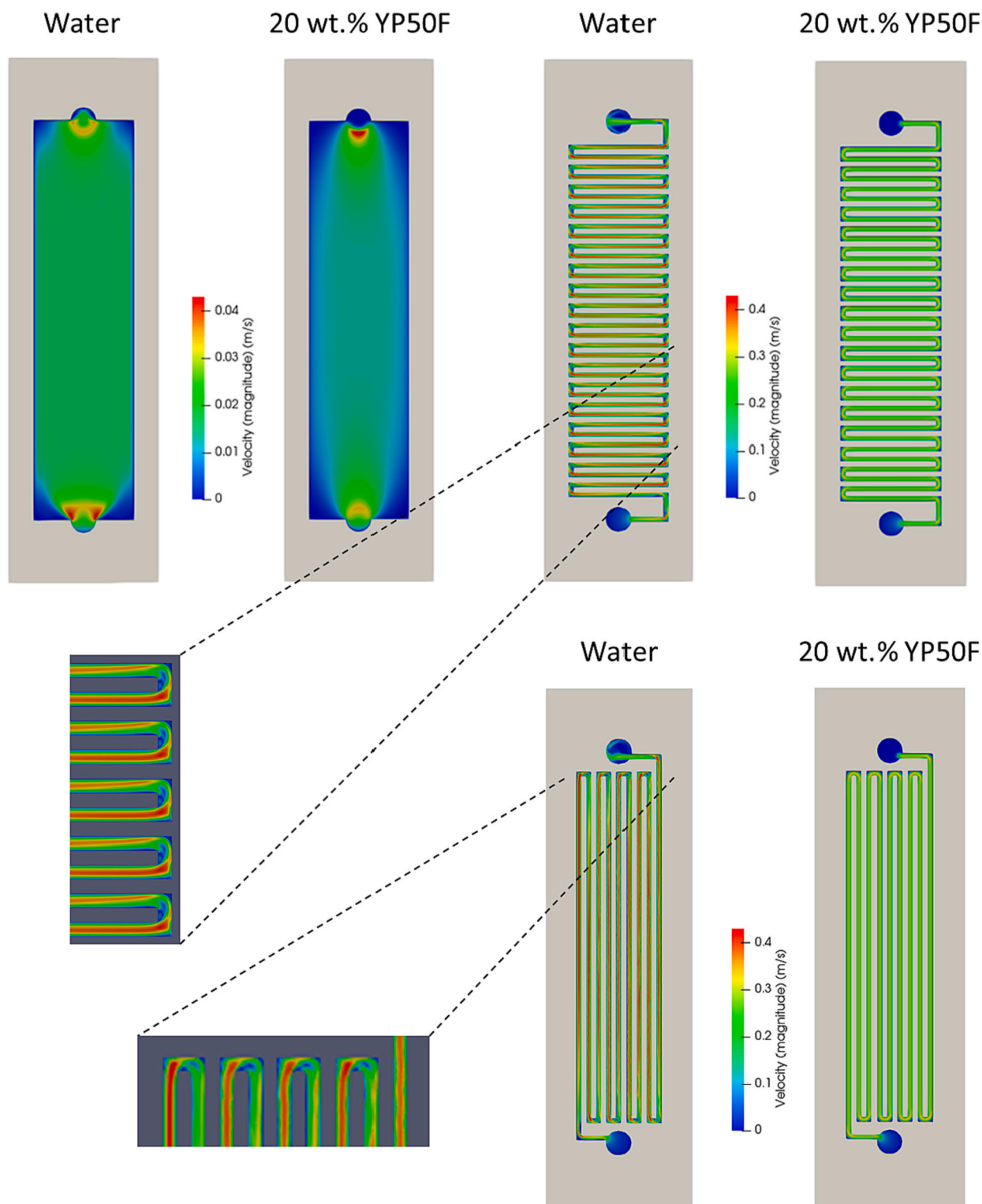


Fig. 6. Slits (at the middle of the channel) of velocity fields (m/s) of water and flow electrode (20 wt% YP50F) in channels with open, serpentine vertical and serpentine horizontal geometries, as predicted by computational fluid dynamics (CFD) simulations.

water) on the left and with serpentine geometry in the middle (for water) and on the right (for flow electrode). For the channel with open geometry, no mixing was predicted, not even with water, which shows, together with viscosity fields, that such geometry is not suitable for use as a flow electrode channel. Streamlines of the flow electrode in the open geometry (figure not shown) were almost the same as for water (thus without any mixing), but the velocity values were slightly lower.

Streamlines in the bends of serpentine vertical and serpentine horizontal channels were very similar, thus only the latter are shown.

When the fluid was water, it is very clear that there is mixing in the bends where streamlines are crossing, although there is no mixing at the straight segments. That mixing at the bends might result due to the formation of Dean eddies. However, when the fluid is the flow electrode, no mixing is predicted, not even at the bends. Also, as observed for the

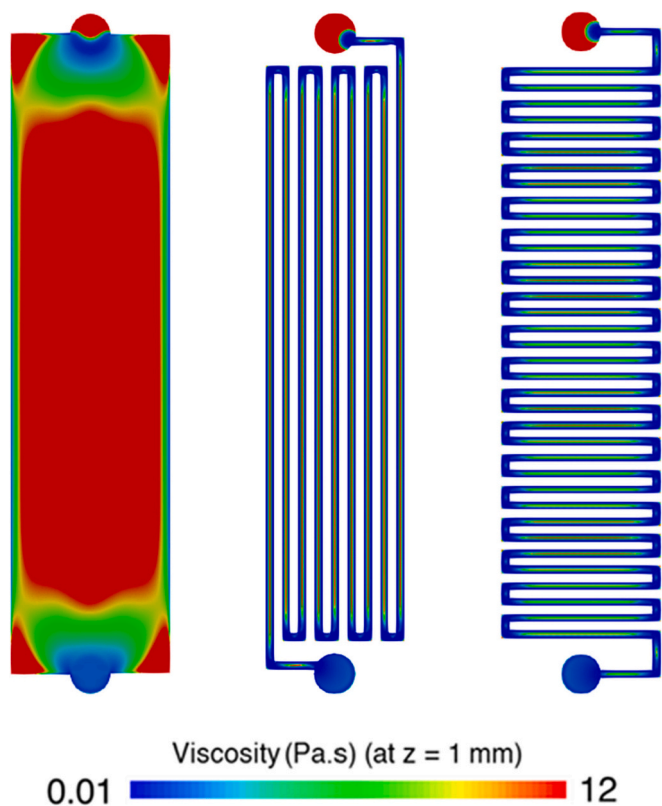


Fig. 7. Slits (at the middle of the channel) of viscosity fields for the flow electrode with 20 wt% of YP50F in channels with open, serpentine vertical and serpentine horizontal geometries, as predicted by computational fluid dynamics (CFD) simulations.

open design, the velocity values are slightly lower for the flow electrode in comparison with the ones observed for water. Since there is no mixing of flow electrodes, even in the bends, only the first layers which are in contact with the current collector are getting charged, thus can electro-sorb ions, which means that it is imperative to develop alternative designs where better mixing of shear-thinning fluids is promoted.

4. Conclusions and perspective

This work demonstrates the profound influence of flow electrode channels geometry and dimensions on the desalination performance of flow capacitive deionization (FCDI). Furthermore, the reverse-voltage desorption (RVD) conditions were found to be the most effective to increase salt removal. Flow electrodes are non-Newtonian fluids with shear-thinning behaviour, *i.e.*, their viscosity decreases with the increase of shear rate, which local values are influenced by the shape (geometry) of channels. Thus, as evidenced by performed CFD simulations, when working with flow electrodes, it is very important to avoid long straight channels without any interposed velocity gradients as it leads to low local shear rate and, therefore, to the increase of flow electrodes viscosity. The most evident consequence of such behaviour was observed when the serpentine vertical (long) channels clogged. Conversely, periodic perturbations of the velocity field, such as bends within the serpentine design, reduce flow electrodes viscosity, thereby facilitating smoother flow, but they must be frequent. This was the case for herein used serpentine horizontal design and, indeed, the FCDI cell employing such gaskets had the highest salt removal. However, and surprisingly, as never reported so far, even though the serpentine geometry (with short channels) stands as the most favourable condition, it fails to promote the internal mixing of flow electrodes. The main key messages and guidelines are:

- The geometry of channels has a strong impact on the internal pressure drop, local shear rate and flow electrodes' viscosity, thus ultimately affecting their flowability.

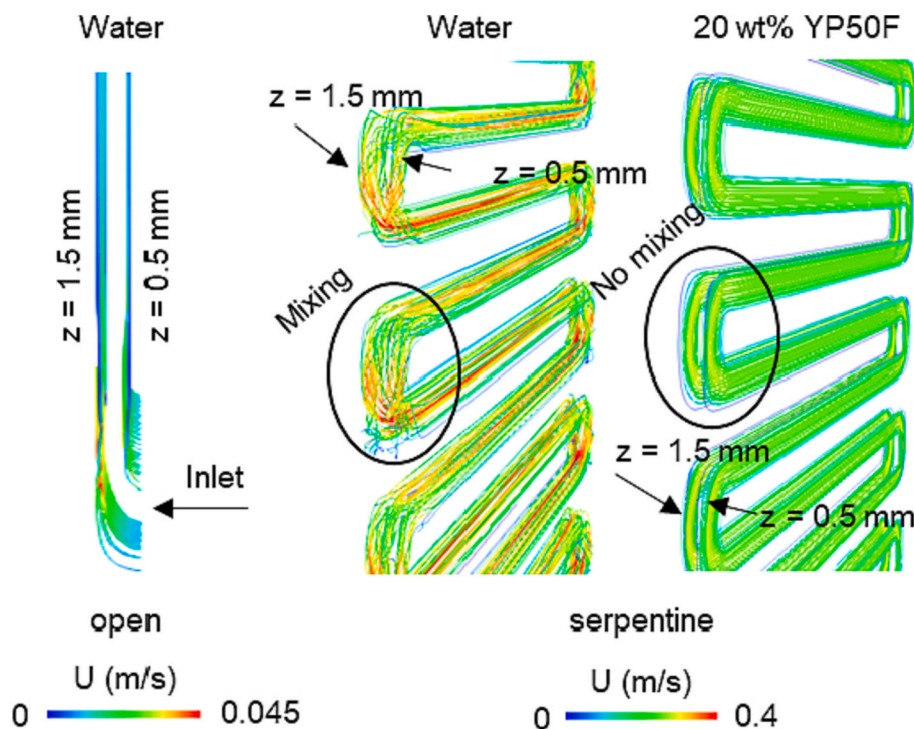


Fig. 8. Representation of streamlines (fluid pathways of water and flow electrode) passing through $z = 0.5$ and 1.5 mm, in channels with open and serpentine horizontal geometries, as predicted by computational fluid dynamics (CFD) simulations.

- The viscosity of flow electrodes in the middle of straight segments increases with the increase of channel length, thus potentially leading to channel clogging issues.
- None of the studied geometries (which are the ones more frequently used in this field) yield efficient internal mixing of flow electrodes. Notably, the formation of Dean vortices was exclusively observed only when water was employed as the working fluid.

Thus, it is still imperative to explore alternative designs that promote effective internal mixing and minimize the viscosity of flow electrodes, especially when performing a scale-up of FCDI, since, as seen here, there is a high risk of clogging of long channels.

CRediT authorship contribution statement

H.M. Saif: Conceptualization, Data curation, Investigation, Methodology, Validation, Visualization, Writing – original draft, Writing – review & editing, Supervision. **T.H. Gebregeorgis:** Investigation, Validation, Visualization, Data curation, Methodology. **J.G. Crespo:** Funding acquisition, Project administration, Resources, Supervision, Writing – review & editing. **S. Pawlowski:** Conceptualization, Data curation, Funding acquisition, Investigation, Methodology, Project administration, Resources, Software, Supervision, Validation, Visualization, Writing – original draft, Writing – review & editing.

Declaration of competing interest

The authors declare that they have no known competing financial interests or personal relationships that could have appeared to influence the work reported in this paper.

Data availability

Data will be made available on request.

Acknowledgments

This work received funding from Fundação para a Ciência e Tecnologia, I.P. (FCDT/MCTES) under grant agreement No PTDC/EQU-EQU/6193/2020 (Se(L)ect(i)ivity) and computational time at Rede Nacional de Computação Avançada through the following advanced computational projects CPCA/A0/401985/2021, CPCA/A1/469450/2021 and 2023.00015.CPCA.A1. This work received funding from the European Union's Horizon 2020 research and innovation programme under grant agreement No 869467 (SEArctularMINE). This work was also supported by the Associate Laboratory for Green Chemistry – LAQV which is financed by national Portuguese funds from FCT/MCTES (UIDB/50006/2020). Tewelde Hailay Gebregeorgis acknowledges the European Commission - Education, Audiovisual and Culture Executive Agency (EACEA) for the Erasmus Mundus scholarship under the program: Erasmus Mundus Master in Membrane Engineering for a Sustainable World (EM3E-4SW), Project Number-574441-EPP-1-2016-1-FR-EPPKA1-JMD-MOB. Hafiz Muhammad Saif Ullah Saleem acknowledges FCT/MCTES for his PhD grant (2020.09828.BD).

Appendix A. Supplementary data

Supplementary data to this article can be found online at <https://doi.org/10.1016/j.desal.2024.117452>.

References

- [1] S. Il Jeon, H.R. Park, J.G. Yeo, S. Yang, C.H. Cho, M.H. Han, D.K. Kim, Desalination via a new membrane capacitive deionization process utilizing flow-electrodes, *Energy Environ. Sci.* 6 (2013) 1471–1475, <https://doi.org/10.1039/c3ee24443a>.
- [2] S. Pawlowski, R.M. Huertas, C.F. Galinha, J.G. Crespo, S. Velizarov, On operation of reverse electrodialysis (RED) and membrane capacitive deionisation (MCDI) with natural saline streams: a critical review, *Desalination* 476 (2020), <https://doi.org/10.1016/j.desal.2019.114183>.
- [3] H.M. Saif, J.G. Crespo, S. Pawlowski, Lithium recovery from brines by lithium membrane flow capacitive deionization (Li-MFCDI) – a proof of concept, *J. Membr. Sci. Lett.* 3 (2023) 100059, <https://doi.org/10.1016/j.memlet.2023.100059>.
- [4] C. Zhang, J. Ma, J. Song, C. He, T.D. Waite, Continuous ammonia recovery from wastewaters using an integrated capacitive flow electrode membrane stripping system, *Environ. Sci. Technol.* 52 (2018) 14275–14285, <https://doi.org/10.1021/acs.est.8b02743>.
- [5] G. Polaranmi, M. Bechelany, P. Sizat, M. Cretin, F. Zaviska, Towards electrochemical water desalination techniques: a review on capacitive deionization, membrane capacitive deionization and flow capacitive deionization, *Membranes* (Basel) 10 (2020), <https://doi.org/10.3390/membranes10050096>.
- [6] E. Avraham, B. Shapira, I. Cohen, D. Aurbach, Electrical double layer in nano-pores of carbon electrodes: beyond CDI; sensing and maximizing energy extraction from salinity gradients, *Curr. Opin. Electrochem.* 36 (2022), <https://doi.org/10.1016/j.coelec.2022.101107>.
- [7] H. Parant, G. Muller, T. Le Mercier, J.M. Tarascon, P. Poulin, A. Colin, Flowing suspensions of carbon black with high electronic conductivity for flow applications: comparison between carbons black and exhibition of specific aggregation of carbon particles, *Carbon* N Y 119 (2017) 10–20, <https://doi.org/10.1016/j.carbon.2017.04.014>.
- [8] Y. Cai, X. Zhao, Y. Wang, D. Ma, S. Xu, Enhanced desalination performance utilizing sulfonated carbon nanotube in the flow-electrode capacitive deionization process, *Sep. Purif. Technol.* 237 (2020), <https://doi.org/10.1016/j.seppur.2019.116381>.
- [9] J.W. Campos, M. Beidaghi, K.B. Hatzell, C.R. Dennison, B. Musci, V. Presser, E. C. Kumbur, Y. Gogotsi, Investigation of carbon materials for use as a flowable electrode in electrochemical flow capacitors, *Electrochim. Acta* 98 (2013) 123–130, <https://doi.org/10.1016/j.electacta.2013.03.037>.
- [10] B. Akuzum, L. Agartan, J. Locco, E.C. Kumbur, Effects of particle dispersion and slurry preparation protocol on electrochemical performance of capacitive flowable electrodes, *J. Appl. Electrochem.* 47 (2017) 369–380, <https://doi.org/10.1007/s10800-017-1046-5>.
- [11] S. Yang, J. Choi, J.G. Yeo, S. Il Jeon, H.R. Park, D.K. Kim, Flow-electrode capacitive deionization using an aqueous electrolyte with a high salt concentration, *Environ. Sci. Technol.* 50 (2016) 5892–5899, <https://doi.org/10.1021/acs.est.5b04640>.
- [12] C. Zhang, L. Wu, J. Ma, A.N. Pham, M. Wang, T.D. Waite, Integrated flow-electrode capacitive deionization and microfiltration system for continuous and energy-efficient brackish water desalination, *Environ. Sci. Technol.* (2019), <https://doi.org/10.1021/acs.est.9b04436>.
- [13] J. Ma, J. Ma, C. Zhang, J. Song, R.N. Collins, T.D. Waite, Water recovery rate in short-circuited closed-cycle operation of Flow-Electrode Capacitive Deionization (FCDI), *Environ. Sci. Technol.* 53 (2019) 13859–13867, <https://doi.org/10.1021/acs.est.9b03263>.
- [14] J. Ma, J. Ma, C. Zhang, J. Song, W. Dong, T.D. Waite, Flow-electrode capacitive deionization (FCDI) scale-up using a membrane stack configuration, *Water Res.* 168 (2020), <https://doi.org/10.1016/j.watres.2019.115186>.
- [15] Z. Zhu, J. Xiong, M. Chen, L. Mu, X. Lu, J. Zhu, Insights into the particle hydrophilicity and electrical conductivity for the construction of a highly efficient electrical percolation network in flow electrode capacitive deionization, *Ind. Eng. Chem. Res.* 62 (2023) 17721–17730, <https://doi.org/10.1021/acs.iecr.3c02260>.
- [16] G. Shen, J. Ma, J. Niu, R. Zhang, J. Zhang, X. Wang, J. Liu, J. Gu, R. Chen, X. Li, C. Liu, Mechanism of ball milled activated carbon in improving the desalination performance of flow- and fixed-electrode in capacitive deionization desalination, *Front. Environ. Sci. Eng.* 17 (2023), <https://doi.org/10.1007/s11783-023-1664-6>.
- [17] X. Zhang, J. Zhou, H. Zhou, H. Zhang, H. Zhao, Enhanced desalination performance by a novel Archimedes spiral flow channel for flow-electrode capacitive deionization, *ACS ES T Eng.* 2 (2022) 1250–1259, <https://doi.org/10.1021/acsestengg.1c00445>.
- [18] S. Yang, S. Il Jeon, H. Kim, J. Choi, J.G. Yeo, H.R. Park, D.K. Kim, Stack design and operation for scaling up the capacity of flow-electrode capacitive deionization technology, *ACS Sustain. Chem. Eng.* 4 (2016) 4174–4180, <https://doi.org/10.1021/acssuschemeng.6b00689>.
- [19] K. Luo, Q. Niu, Y. Zhu, B. Song, G. Zeng, W. Tang, S. Ye, J. Zhang, M. Duan, W. Xing, Desalination behavior and performance of flow-electrode capacitive deionization under various operational modes, *Chem. Eng. J.* 389 (2020), <https://doi.org/10.1016/j.cej.2020.124051>.
- [20] J. Ma, C. He, D. He, C. Zhang, T.D. Waite, Analysis of capacitive and electrochemical contributions to water desalination by flow-electrode CDI, *Water Res.* 144 (2018) 296–303, <https://doi.org/10.1016/j.watres.2018.07.049>.

- [21] M. Wang, S. Hou, Y. Liu, X. Xu, T. Lu, R. Zhao, L. Pan, Capacitive neutralization deionization with flow electrodes, *Electrochim. Acta* 216 (2016) 211–218, <https://doi.org/10.1016/j.electacta.2016.09.026>.
- [22] A. Ambrosi, M. Pumera, 3D-printing technologies for electrochemical applications, *Chem. Soc. Rev.* 45 (2016) 2740–2755, <https://doi.org/10.1039/c5cs00714c>.
- [23] M.P. Browne, E. Redondo, M. Pumera, 3D printing for electrochemical energy applications, *Chem. Rev.* 120 (2020) 2783–2810, <https://doi.org/10.1021/acs.chemrev.9b00783>.
- [24] S. Pawlowski, J.G. Crespo, S. Velizarov, Pressure drop in reverse electrodialysis: experimental and modeling studies for stacks with variable number of cell pairs, *J. Membr. Sci.* 462 (2014) 96–111, <https://doi.org/10.1016/j.memsci.2014.03.020>.
- [25] S. Pawlowski, P. Sizat, J.G. Crespo, S. Velizarov, Mass transfer in reverse electrodialysis: flow entrance effects and diffusion boundary layer thickness, *J. Membr. Sci.* 471 (2014) 72–83, <https://doi.org/10.1016/j.memsci.2014.07.075>.
- [26] K.B. Hatzell, M.C. Hatzell, K.M. Cook, M. Boota, G.M. House, A. McBride, E. C. Kumbur, Y. Gogotsi, Effect of oxidation of carbon material on suspension electrodes for flow electrode capacitive deionization, *Environ. Sci. Technol.* 49 (2015) 3040–3047, <https://doi.org/10.1021/es5055989>.

Supplementary Information to:

The influence of flow electrode channel design on flow capacitive deionization performance: Experimental and CFD modelling insights

H.M. Saif¹, T.H. Gebregeorgis^{1,**}, J.G. Crespo^{1,2}, S. Pawlowski^{1,*}

¹LAQV-REQUIMTE, DQ, FCT, Universidade NOVA de Lisboa, 2829-516 Caparica, Portugal

²Instituto de Tecnologia Química e Biológica António Xavier, Universidade Nova de Lisboa, Av. da República, 2780-157 Oeiras, Portugal

*Corresponding author: E-mail: s.pawlowski@fct.unl.pt (Sylwin Pawlowski)

**Current address: Research Group Electrochemical and Surface Engineering (SURF), Department of Materials and Chemistry, Vrije Universiteit Brussel (VUB), Pleinlaan 2, 1050 Brussels, Belgium

1) 3D printing of flow electrode gaskets

Table SI.1. Tested conditions for producing PET-G-made flow electrode gaskets.

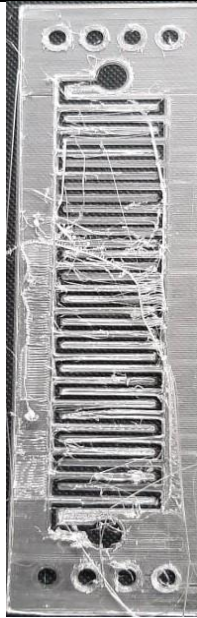
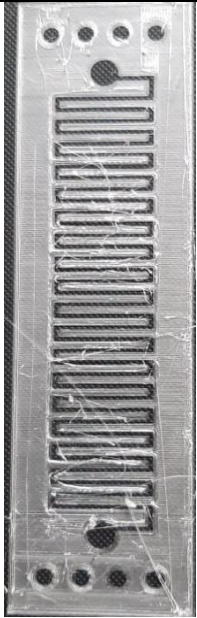
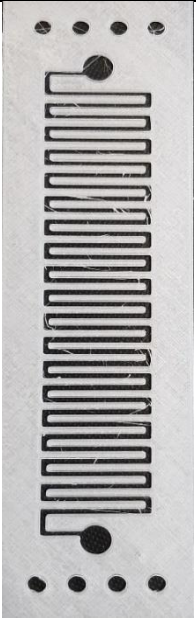
Print Case	A	B	C	D	E
Nozzle temperature	235°C	200°C	220°C	210°C	210°C
Infill print speed	36 mm/s	48 mm/s	48 mm/s	48 mm/s	36 mm/s
Print:					

Table SI.2. 3D printing conditions used to manufacture flow electrode gaskets.

Printing parameter		Printing parameter	
Filament	PET-G	Height maximum multiplier	0.85
Quality	100%	First layer height	0.25 mm
Durability	Light	First layer extrusion	110%
Infill	30%	Filament diameter	1.75 mm
Support	No	Extrusion multiplier	1
Print speed	30 mm/s	Hot bed temperature	60°C
Travel speed	90 mm/s	Extruder temperature	210°C
Infill print speed	150%	Fan speed	100%
Artifact print speed	150%	Retraction height	0.05 mm
First layer speed	40%	Retraction amount	2 mm
Small perimeter speed	70%	Retraction speed z	10 mm/s
Small perimeter threshold	20 mm	Retraction speed e	100 mm/s
Maximum adhesion ratio	2	Wipe distance	2 mm
Height minimum multiplier	0.3	Retract on start	1

Table SI.3. Time taken to print the flow electrode gaskets.

Gasket geometry	Job time (hours: minutes: seconds)	PET-G filament length
Open	2:34:56	6.16 meter
Horizontal serpentine	5:03:09	9.95 meter
Vertical serpentine	5:02:57	10.20 meter

2) FCDI desalination tests lab setup and FCDI cell interior parts.

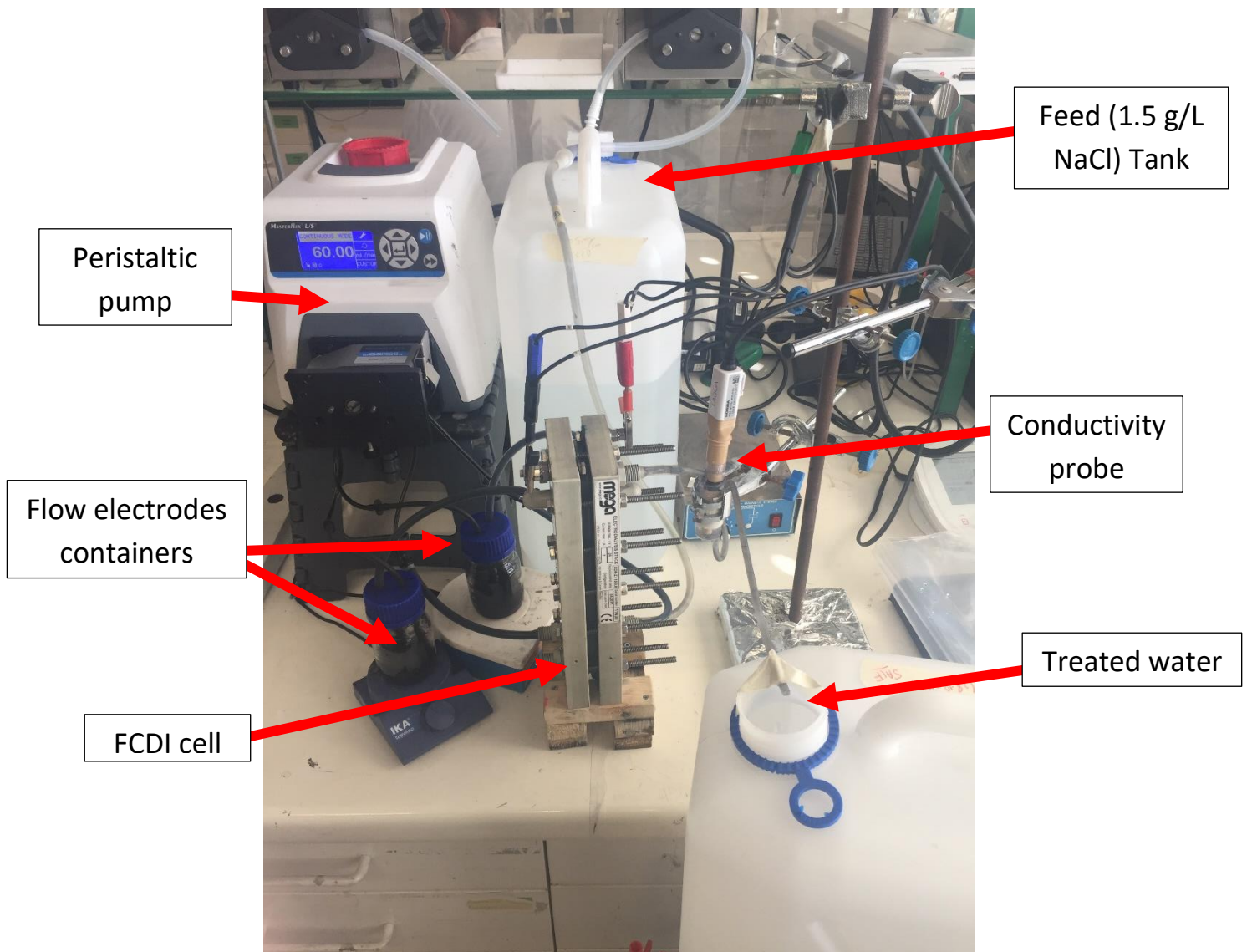


Fig. SI.1. FCDI setup used in this work.

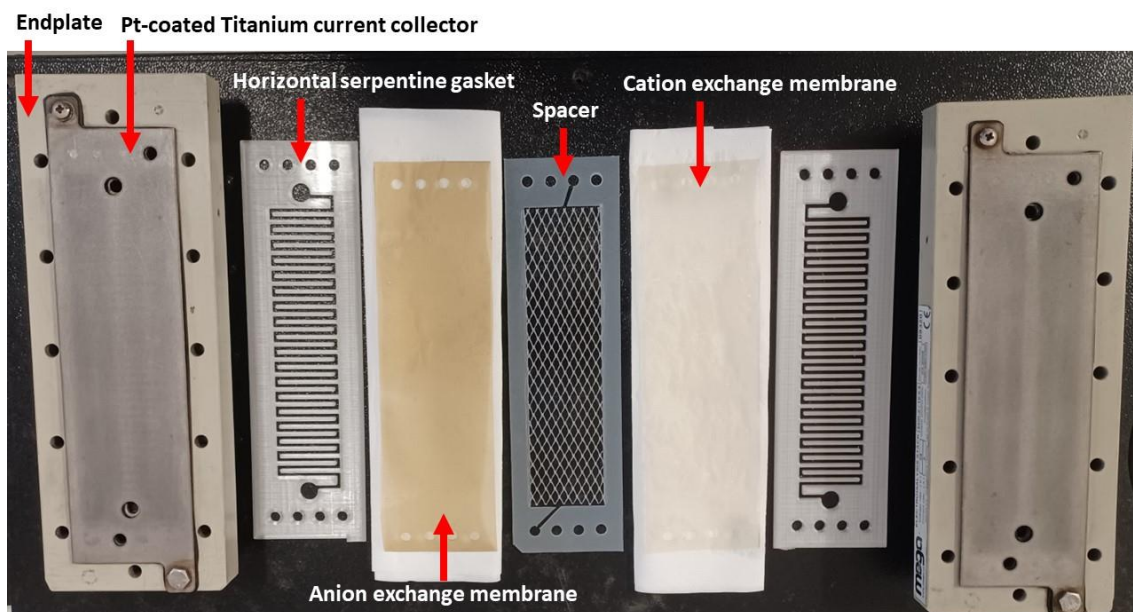


Fig. SI.2. Components of the FCDI cell with horizontal serpentine gaskets.

3) Pressure drop in flow electrode channels

Table SI.4. Pressure drop values at a flow rate of 60 ml/min of water and 20 wt.% YP50F flow electrode in open, serpentine vertical and serpentine horizontal channels. The error of measurement is ± 5 mbar.

Geometry\Fluid	Water (mbar)	20 wt.% YP50F (mbar)
Open	5	20
Vertical	10	25*
Horizontal	30	75

* Values obtained while channels haven't yet clogged.

4) Effect of carbon loading

To investigate the effect of carbon loading, desalination tests with flow electrode with 0 wt.% (so just 1 g/L NaCl solution), 5 wt.%, 10 wt.% and 15 wt.% of AC were performed in a single pass experiment, at $\pm 1V$, thus under reverse voltage desorption (RVD) conditions, and each step time of 150 s. The feed flow rate and concentration were 10 ml/min and 1.5 g/L NaCl, respectively, the electrode flow rate was 60 ml/min, and horizontal serpentine flow electrode gaskets were used. The results are shown in terms of current–time (Figure SI.3), salt removal (Figure SI.4) and salt adsorption capacity (Figure SI.5) at the last adsorption step (5th cycle).

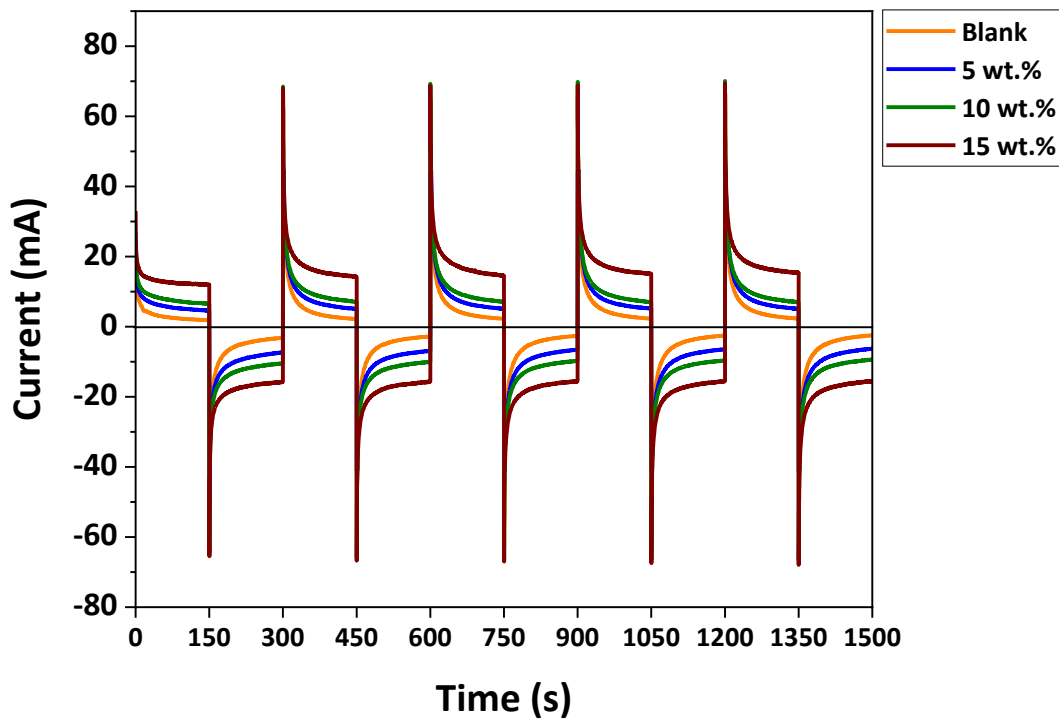


Fig. SI.3. Profiles of electric current during FCDI desalination tests, with horizontal serpentine gaskets, under RVD conditions ($\pm 1V$), when using flow electrodes with different carbon loading.

Figure SI.3 shows that with the increase of carbon loading in flow electrodes, a higher electric current is obtained in the FCDI cell, thus more ions are transported, which translates into an increase of the quantity of salt which is removed (Figure SI.4).

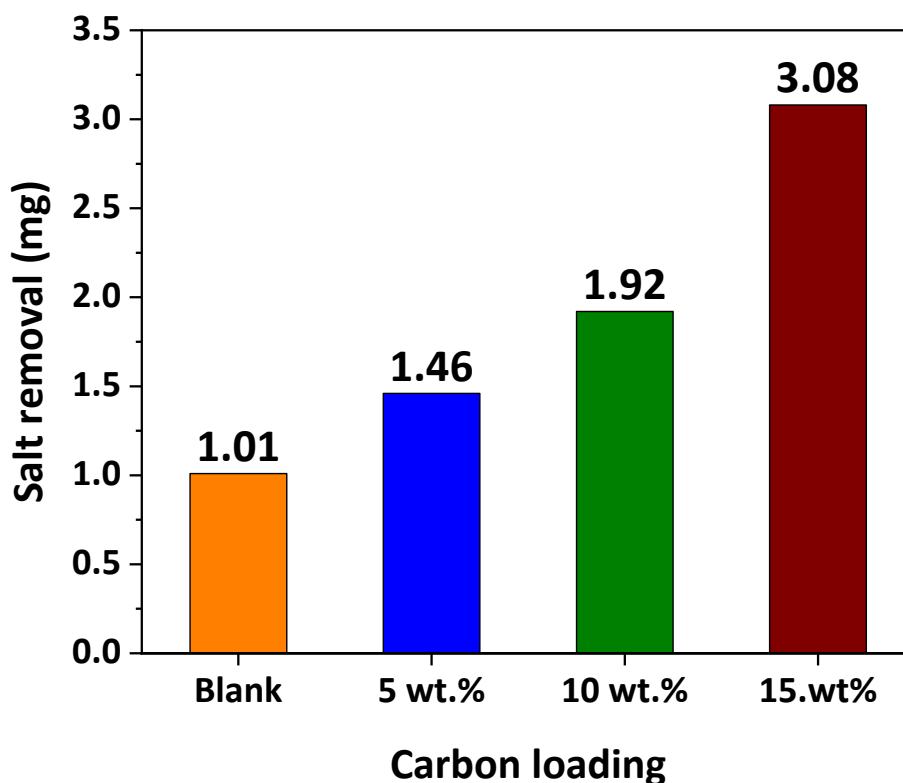


Fig. SI.4. Salt removal at the 5th adsorption step of 150 s during FCDI desalination tests, with horizontal serpentine gaskets, under RVD conditions ($\pm 1V$), when using flow electrodes with different carbon loading.

The highest amount of salt (3.08 mg during 150 s) was removed when flow electrodes with 15 wt.% AC were used, which is more than 3 times higher amount when compared with the blank test (without any carbon in the anode and cathode compartments, thus operated as an electro dialysis stack).

To investigate how effectively the activated carbon material is used in the flow electrodes during the desalination test, the salt adsorption capacity (SAC) was calculated (Figure SI.5).

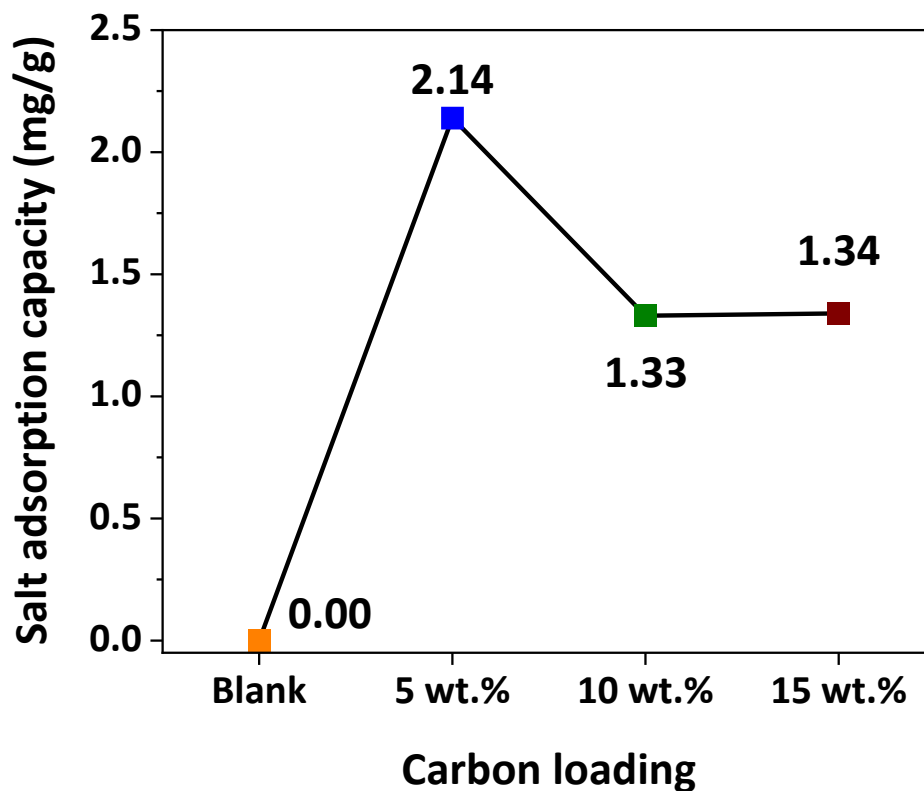


Fig. SI.5. Salt adsorption capacity (SAC) at the 5th adsorption step of the used flow electrode as calculated from the performance of FCDI cells, with horizontal serpentine gaskets, under RVD conditions ($\pm 1V$), when using flow electrodes with different carbon loading.

The highest SAC was achieved when flow electrodes with 5 wt.% of AC were used, which indicates the most effective utilization of the carbon material. On the other hand, the SAC values for 10 wt.% and 15 wt.% AC slurries were almost the same. This behaviour might arise from better mixing of flow electrodes with 5 wt.% of AC since they have the lowest

viscosity. With the increase of carbon loading, the viscosity increases, reaching a point at which there is no internal mixing, hence SAC decreased and eventually stabilized. Therefore, in order to achieve a relatively high salt removal, at acceptable SAC values, and at a relatively low viscosity of flow electrodes (to operate the FCDI process without risk of channels clogging), a flow electrode with 10 wt.% of activated carbon was used to analyse the effect of flow electrode channel design on the FCDI desalination performance. Even so, as reported in the manuscript, the vertical serpentine channels clogged, which was then thoroughly investigated through CFD simulations.